Cochlear Mechanics

Academic and Research Staff
Professor Dennis M. Freeman, Dr. Alexander Aranyosi

Graduate Students
Shirin Farrahi, Roozbeh Ghaffari, Scott Page

Longitudinally Propagating Traveling Waves of the Tectorial Membrane

Sponsors
National Institutes of Health Grant R01 DC00238

Project Staff
Roozbeh Ghaffari, Dr. Alexander Aranyosi, Professor Dennis M. Freeman

Introduction

The mammalian cochlea is a remarkable sensor that can detect motions smaller than the diameter of a hydrogen atom and can perform high-quality spectral analysis to discriminate as many as 30 frequencies in the interval of a single semitone (Kossl and Russell, 1995; Dallos, 1996). These extraordinary properties of the hearing organ depend on traveling waves of motion that propagate along the basilar membrane (BM) (von Bekesy, 1960) and ultimately stimulate the sensory receptors. There are two types of cochlear receptors: the inner and outer hair cells (OHCs). Both types of hair cells contain densely packed arrays of stereocilia called hair bundles that transducer mechanical energy into electrical signals (Hudspeth, 1985). These hair bundles project from the apical surface of hair cells toward an overlying gelatinous matrix called the tectorial membrane (TM).

The strategic anatomical configuration of the TM relative to the hair bundles suggests that the TM plays a key role in stimulating hair cells. Mouse models with genetically modified structural components of the TM have been shown to exhibit severe loss of cochlear sensitivity and altered frequency tuning (McGuirt et al, 1999; Legan et al, 2000; Simmler et al, 2000; Legan et al, 2005; Russell et al, 2007), thereby providing further evidence that the TM is required for normal cochlear function. However, the mechanical processes by which traveling wave motion along the BM leads to hair cell stimulation remain unclear (Guinan et al, 2005), largely because the important mechanical properties of the TM have proved difficult to measure. Consequently, the mechanical function of the TM has been variously described as a rigid pivot, a resonant structure, and a free-floating mass (Davis, 1958; Allen, 1980; Zwislocki, 1980; Mammano and Nobili, 1993) in “classical” cochlear models, which assume that adjacent longitudinal sections of the cochlear are uncoupled except for energy propagation through the fluid (de Boer, 1997). Recent measurements have shown that the TM is viscoelastic (Abnet and Freeman, 2000) and can couple motion over significant longitudinal cochlear distances (Abnet and Freeman, 2000; Russell et al, 2007), suggesting that the TM also may support waves. Here we show that longitudinally propagating traveling waves are intrinsic to the material properties of the mammalian TM (Ghaffari et al, 2007). The longitudinal extent of wave motion suggests that TM waves can stimulate hair cells from multiple regions of the cochlea and interact with the BM traveling wave to affect cochlear function.

Traveling wave motions of the TM

To study wave propagation in the TM, we developed an experimental chamber in which a segment of an isolated TM from the mouse cochlea is suspended between two parallel-aligned

supports in artificial endolymph (figure 1A). Sinusoidal forces applied in the radial direction at one support launched waves that propagated longitudinally along the TM toward the other support (figure 1B). These waves were generated with nanometer-scale amplitudes (≈ 90–400 nm) over a broad range of frequencies (1–20 kHz). An optical imaging system synchronous with the driving stimulus (Aranyosi and Freeman, 2004) tracked radial displacement amplitude and phase at multiple points on the surface of the TM.

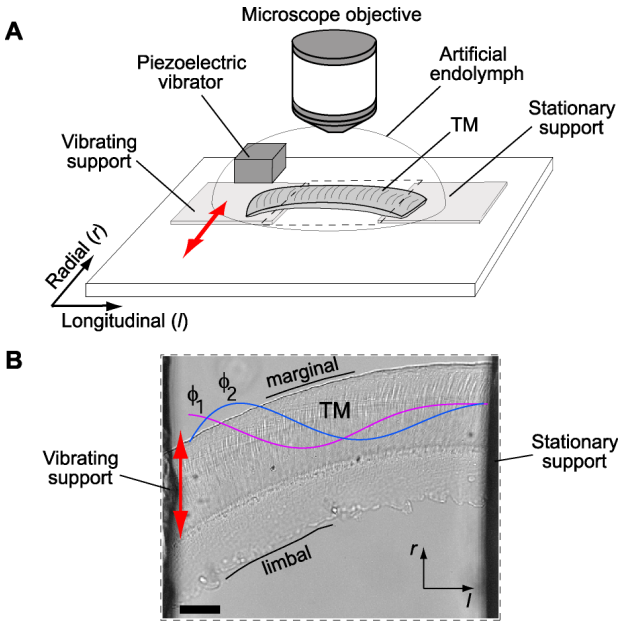

Figure 1: Suspended TM segment in wave chamber. **A**. Schematic of TM segment suspended between two supports (not to scale). Double headed arrow indicates sinusoidal displacement of vibrating support at audio frequencies. Radial displacement of the TM was tracked at audio frequencies by using stroboscopic illumination. **B**. Image of TM segment taken with a light microscope. (Scale bar, 50 μm) Displacement and phase of propagating motion were tracked at several points along the TM in the region that normally overlies the hair bundles. Marginal and limbal boundaries of the TM are indicated. The two schematic waveforms pasted on the image are displacement snapshots at sequential instants (Φ_1, Φ_2) illustrating typical TM deformations. Displacement amplitudes were exaggerated to show wave-like nature of the motion.

Figure 2A shows the spatial pattern of radial displacement of a typical basal TM segment in response to 15 kHz motion of the vibrating support. The measurements were well fit by an exponentially decaying sinusoid, corresponding to a wave with wavelength of 350 μm and wave decay constant of 240 μm. TM wave motion scaled linearly with applied displacement at the vibrating support and wavelengths were constant over the range of displacements applied to the TM (~ 90–340 nm).

The phase of radial displacement varied with longitudinal distance in a frequency-dependent manner. In figure 2B, the phase at low frequencies (2 kHz) reached $\pi/6$ radians over the length of the suspended TM. In contrast, at high frequencies (≥ 18 kHz), the phase lag exceeded a complete cycle (> 2π radians). Phase also was measured as a function of stimulus frequency location on the surface of the TM ≈ 250 μm from the vibrating support. Figure 2C shows that phase lag increased with stimulus frequency. This trend was evident across all TM samples, and the lag was larger for TM segments from the apical turn of the cochlea than for segments from the basal turn.

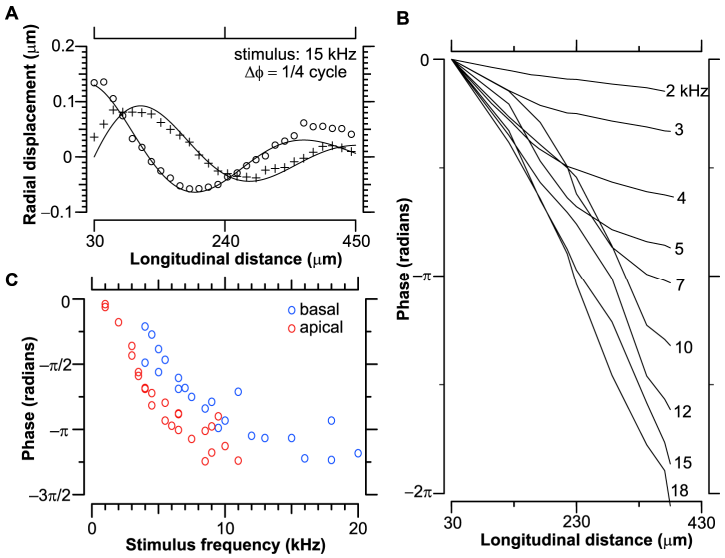

Figure 2: A. TM radial displacement vs. longitudinal distance in response to 15 kHz stimulation of vibrating support. Solid lines represent exponentially decaying sinusoid fit to the measurements at 16 equally spaced stimulus phases (two shown separated by ¼ cycle). **B.** Phase vs. longitudinal distance for stimulus frequencies 2–18 kHz. Phase lag increased monotonically with distance and became steeper with increasing frequency. Phase was measured relative to a point on the surface of the TM ~ 30 μm from the vibrating support. **C**. Phase vs. stimulus frequency at a location on the surface of the TM ≈ 250 μm from vibrating support. Apical TMs (red; *n* = 25 measurements) accumulated more phase lag than basal TMs (blue; *n* = 22 measurements). The entire data set represents measurements across six TM preparations (three basal and three apical TMs).

The velocity of wave propagation v_s was computed for basal and apical TM segments as the product of frequency and wavelength for each stimulus frequency. TM wave velocity values ranged from 2–10 m/s and increased with stimulus frequency (figure 3A). The propagation velocities of the TM wave are strikingly similar to those of the BM wave near the best place (figure 3B). Furthermore, waves propagated towards the stationary support with these velocities when either the basal or apical end of the TM segment was attached to the vibrating support, indicating that both forward and reverse traveling waves propagate through the TM.

Previously the material properties of the TM were shown to be viscoelastic over a broad range of frequencies (Abnet and Freeman, 2000; Gu et al, 2008). For pure shear waves in an infinite, isotropic, viscoelastic material, v_s is related to the shear storage modulus G' and the shear viscosity η by

$$v_s = \sqrt{\frac{2(G'^2 + \omega^2\eta^2)}{\rho(G' + \sqrt{G'^2 + \omega^2\eta^2})}} \qquad (1)$$

where ω is the angular frequency of vibration and ρ is the density of the material, assumed to be equal to that of water (Chen et al, 2004). This equation suggests that the velocity should increase with frequency, as was seen in figure 3A, and implies that the interaction of TM inertial and shear properties give rise to traveling waves.

A

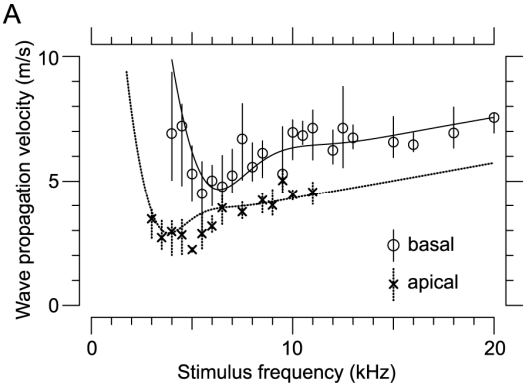

B

Species	Distance from base, mm (%Length)	CF, kHz	Velocity, m/s
Gerbil	1.6 (14)	25	22.5
Guinea pig	1.7 (9)	31	28
Guinea pig	4 (22)	15	10
Guinea pig	5-6.5 (27-35)	5-9	5-6
Guinea pig	12.8 (69)	1	1.55
Cat	2.6 (10)	31	19
Chinchilla	2.6 (14)	12	6
Chinchilla	2.7 (15)	10	6
Chinchilla	14 (76)	0.62	0.76
Squirrel monkey	9 (39)	6.5	12

Compiled by Robles and Ruggero, 2001

Figure 3: Propagation velocity of TM traveling waves compared to BM waves. **A.** Propagation velocity of TM waves vs. stimulus frequency. Symbols represent the median values of propagation velocity measured across multiple frequencies for basal (o) and apical (x) segments. Interquartile ranges are represented with vertical lines. Fit lines represent model predictions of v_s vs. frequency for typical basal (solid) and apical (dotted) TM samples. **B.** BM wave propagation velocities near BF locations across different species (Table adapted from Robles and Ruggero, 2001). TM waves propagate with velocities (2–10 m/s) that are comparable to those of the BM traveling wave.

To account for the finite cross-section of the TM, the finite length of the wave chamber, and the effect of surrounding fluid, we analyzed a finite difference model of the TM (Ghaffari et al, 2007). The model consisted of a longitudinally distributed series of masses coupled by viscous and elastic elements. The radial displacements of the TM at the vibrating and stationary supports were constrained in the model as they were in the wave chamber. The measurements of v_s were fit by this model for both basal and apical TM segments. The best fit of this model to TM wave displacements predicted material properties for basal (G' = 47 ± 12 kPa; η = 0.19 ± 0.07 Pa·s; n = 5) and apical (G' = 17 ± 5 kPa; η = 0.15 ± 0.05 Pa·s; n = 3) TM segments that are remarkably similar to those determined using an independent method (Gu et al, 2008).

The finite difference model also showed that the TM can support waves in the presence of cochlear loads, such as hair bundle stiffness, the limbal attachment, and damping in the subtectorial space (Ghaffari et al, 2007). We assumed a nominal hair bundle stiffness of 3.5 mN/m was evenly distributed across an 8 μm extent of the TM for each of the three rows of OHCs. Adding hair bundle stiffness increased the wave decay constants by 1%. We modeled the limbal attachment as a local stiffness load. The effect of the limbal attachment was apparent only for sufficiently large stiffnesses, which caused the wavelength and wave decay constant to increase by 10–15%. Damping in the subtectorial space was estimated assuming that fluid flow was Couette. Viscous damping in the subtectorial space did not cause significant dissipation even for gaps as small as 1 μm. This result is striking, since such damping has been modeled as the primary loss mechanism in the cochlea (Allen, 1980).

Implications for Cochlear Mechanics

The waves reported in this study provide evidence for significant spatial coupling through cochlear structures. This finding counters a fundamental assumption in classical cochlear macromechanical models: that adjacent longitudinal sections of the cochlea are coupled through the fluid alone (de Boer, 1996). This finding also counters a fundamental assumption in classical micromechanical models: that micromechanics are local, depending on motions of only adjacent structures. Instead, the presence of both BM and TM waves in the cochlea (figure 4) offers entirely new ways to think about cochlear mechanics. We briefly describe three possibilities.

Otoacoustic Emissions are thought to arise from retrograde BM traveling waves or compressive

fluid waves. Retrograde TM waves could also contribute to cochlear emissions.

Traveling Wave Amplification of two coupled anterograde traveling waves has been described theoretically as a mechanism for cochlear amplification (Hubbard, 1993). Anterograde TM waves are a logical substrate for the second wave.

Recirculating Amplification is made possible by anterograde propagation of BM waves driving retrograde propagation of TM waves. This idea provides a natural mechanism by which amplification basal to the best place can be coupled into a feedback system. In this regard, it is important to note that wave decay constants of the TM span regions of the cochlea with frequencies that vary by 0.5 to 1.0 octaves.

These possibilities illustrate some ways by which TM waves can fundamentally change the way we think about cochlear mechanics.

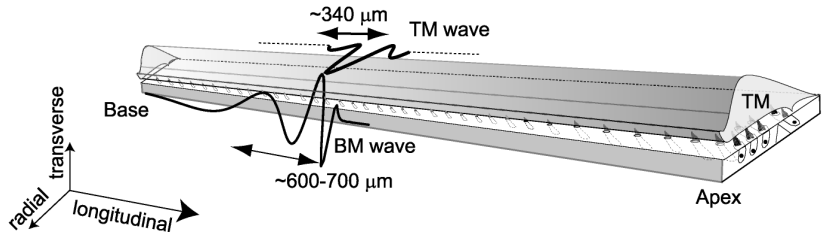

Figure 4: Schematic drawing illustrating the concept that the cochlea supports two traveling waves. TM wave (Top) and BM wave (bottom) both propagate longitudinally with comparable wavelengths and velocities near the BF place. The observed TM waves are longitudinally propagating waves of radial motion; the BM waves are longitudinally propagating waves of transverse motion. These two waves can be coupled through the OHCs and cochlear fluids.

Publications

Journal Articles, Published

Ghaffari, R., A. J. Aranyosi, and D. M. Freeman, “Longitudinally propagating traveling waves of the mammalian tectorial membrane,” *PNAS* **104**:16510-15, 2007.

Gu, J. W., W. Hemmert, D. M. Freeman, and A. J. Aranyosi, “Frequency-dependent shear impedance of the tectorial membrane,” *Biophys J* **95**:1529-38, 2008.

Meeting Papers, Published

Ghaffari, R., A. J. Aranyosi, and D. M. Freeman, “Longitudinally propagating traveling waves of the mammalian tectorial membrane,” presented at the *Thirty-First Annual Midwinter Meeting of the Association for Research in Otolaryngology*, Phoenix, Az, 2008.

Aranyosi, A. J., R. Ghaffari, and D. M. Freeman, “A distributed impedance model of tectorial membrane traveling waves,” presented at the *Thirty-First Annual Midwinter Meeting of the Association for Research in Otolaryngology*, Phoenix, Az, 2008.

Theses

Ghaffari, Roozbeh, *The functional role of the mammalian tectorial membrane in cochlear mechanics*, Ph.D. Thesis, Harvard-MIT Division of Health Sciences and Technology: MIT 2008.